ACS Catalysis

Research Article

pubs.acs.org/acscatalysis

Effects of Gas Feed Ratios and Sequence on Ethylene Hydrogenation on Powder Pt Catalyst Studied by Sum Frequency Generation and Mass Spectrometry

Avishek Ghosh,*[,†] Bryan B. Hsu,[‡] Shawn M. Dougal, Mobae Afeworki, Paul A. Stevens, and Mohsen S. Yeganeh

ExxonMobil Research and Engineering Company, 1545 Route 22 East, Annandale, New Jersey 08801, United States

Supporting Information

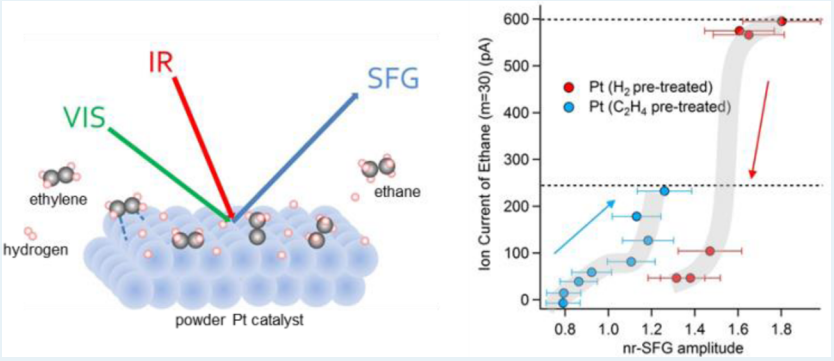

ABSTRACT: The effects of reactant feed ratios and sequences on ethylene hydrogenation over pellets of Pt powder have been studied using sum frequency generation spectroscopy (SFG) and mass spectrometry (MS) at room temperature and atmospheric pressure. Ethylene hydrogenation is shown to depend not only on the feed ratio but also on the sequence of feed gas injection, which affects the competitive adsorption of reactants (H_2, C_2H_4) and various hydrocarbonaceous intermediates on the catalyst surface. Ethane production was highest when the catalyst was pretreated with hydrogen but diminished with increasing amounts of ethylene. At >2:1 (C_2H_4/H_2) feed ratios, ethane generation was at its lowest, and the SFG spectra of the catalyst surface indicate formation of ethylidyne, di-σ-ethylene, and ethylidene, species that block the Pt surface active sites. We demonstrate that it is possible to partially recover the active sites by flowing H_2 through the reactor, although ethane generation was reduced by approximately a factor of 3. Trends in nonresonant SFG (nr-SFG) have been observed to be indicative of H_2 adsorption on the Pt surface and are dependent on the sequence of the feed gas injection, as well. We have revealed correlations between nr-SFG and MS ion current of catalytically generated ethane at various pretreatments of the Pt powder surface, thus demonstrating nr-SFG as a sensitive tool to measure catalytic activity of metal surfaces.

KEYWORDS: *ethylene hydrogenation, ethylene-to-hydrogen ratio, powder catalyst, gas−solid interface, sum frequency generation spectroscopy, nonresonant SFG, surface electronic structure, catalytic activity, heterogeneous catalysis*

INTRODUCTION

Heterogeneous catalytic reactions utilizing an ever-growing variety of metal catalysts have revolutionized a number of industrial chemical processes,[1] although the molecular mechanisms and the chemistries of these reactions are often too complex to be clearly understood. The problem is attributed in part to the general complexity intrinsic to surfaces and in part to the lack of experimental techniques that can directly detect and monitor chemistries with enough surface specificity and signal strengths. The deceptively simple reaction of ethylene hydrogenation over transition metal catalysts, such as Pt and Pd, has been studied for almost a century[2] as a model reaction to understand the rich and complex chemistry metal surfaces have to offer.[3−5] The mechanistic pathway of ethylene hydrogenation on Pt was first laid out by Horiuti and Polanyi in the 1930s.[6] Since then, many experimental techniques have been utilized to study the mechanism under a variety of conditions, elucidate the role of various surface intermediates, and understand the nature and role of catalyst surfaces. In recent decades, with the advent of a number of surface-specific experimental techniques such as LEED,[7,8] HREELS,[9−11] FT-IR,[12−14] reflection absorption infrared spectroscopy (RAIRS),[15−17] and sum frequency generation (SFG),[18−25] enormous progress has been made in our understanding of surface reaction mechanisms. Parallel efforts in microkinetic modeling of the surface reaction kinetics and thermodynam-

Received: January 23, 2014
Revised: April 28, 2014
Published: May 7, 2014

ics,[26,27] along with DFT studies[28−30] of surfaces, have substantiated our understanding of surface phenomena and processes.

Catalytic ethylene hydrogenation involves competitive adsorption of ethylene (C_2H_4) and hydrogen (H_2) on a Pt surface, followed by elementary reactions between the adsorbed transient intermediates, leading to the final product, ethane (C_2H_6). At equilibrium, the sequence of reactant adsorption onto the catalyst would not matter if the adsorption energies and sticking probabilities of the reactants, intermediates, or products on the solid surface were similar. However, if the adsorption energies/sticking probabilities vary widely, one would expect efficiency of the reaction to be very sensitive to the sequence of feed gases. Adsorbed intermediates or products that are difficult to remove from the surface are anticipated to affect the number of active sites of the catalyst, thereby affecting the overall efficiency of the catalytic process. Despite the importance of the competitive adsorption mechanism in a catalytic reaction, our understanding is still evolving. In this paper, we report our findings using sum frequency generation spectroscopy and mass spectrometry (MS), which illustrate the effect of reactant feed sequences on surface intermediates and on the overall ethylene hydrogenation process. We have also explored the effects of reactant feed sequences on the electronic structure of the metal surface, which we anticipate to be a sensitive probe for its catalytic activity.

In the recent past, ethylene hydrogenation on single-crystal Pt(111) has been studied extensively, and the surface intermediates have been well-characterized under various temperatures and pressures. Ethylidyne (Pt_3CCH_3), di-σ-C_2H_4, ethylidene (Pt_2CHCH_3), vinyl, and vinylidene intermediates have been observed as the primary intermediates on the Pt surface under different temperatures and, mostly, at ethylene-rich conditions.[8,11,14,15,18−20] Ethylidyne is claimed to be a spectrator species[19,20] on the Pt surface in the hydrogenation reaction because it does not actively participate in the conversion of ethylene to ethane. However, ethylidyne acts as a surface inhibitor, thus affecting the overall reaction. The ethyl ($PtCH_2CH_3$) intermediate, although very difficult to detect because of its short surface lifetime owing to a fast back-conversion to C_2H_4, has been directly observed by Frei et al. using transmission FT-IR with a pulsed gas feed[12,13] to be the primary precursor to ethane generation in a H_2-rich environment. The pulsed gas feed method allows detection of the surface IR signals with reduced interference from the bulk gas phase signals, which can easily overwhelm the IR surface signals in a steady-state experiment.

In contrast to FT-IR, SFG spectroscopy does not suffer from bulk interference; however, to our knowledge, most prior SFG experiments were performed on crystalline Pt(111) surfaces with a uniform monolayer of surface species to generate detectable surface SFG signals. Under the electric dipole approximation, SFG is an allowed process at the surface of a Pt crystal or even large-sized particles, as long as the center of inversion symmetry is absent. However, commercial and practical heterogeneous catalysts are rarely single crystals and are often small-sized particles ($\ll$1 μm). Therefore, studying interfacial phenomena of commercial powder catalysts is very important and could, in fact, be very different from single crystal studies because of local surface heterogeneities and a large number of surface defects. It is challenging to perform SFG experiments on powders because, with very small sized particles, the sum frequency (SF) photons generated from either side of each particle interfere destructively, making SFG virtually impossible to detect. However, recently, we have demonstrated that the E fields of the incident IR and visible laser beams can be manipulated by employing a total internal reflection geometry using a prism over the catalyst in a way that SF photons from the surface of a powder catalyst become detectable at the critical angle of a catalyst/prism interface.[31]

In our experimental efforts, we have studied ethylene hydrogenation on the surface of pelletized Pt powder using a combination of SFG and mass spectroscopy (MS). Here, we have explored effects of H_2 and C_2H_4-pretreated Pt on the overall ethylene hydrogenation reaction and on various surface intermediates at various gas feed ratios. We followed the effects of feed sequences and feed ratios on the surface intermediates by monitoring the vibrational resonances of various surface hydrocarbons in the SFG spectra while ethane generation was simultaneously monitored by MS. We have demonstrated that production of ethane on Pt at room temperature is sensitive not only to the ethylene/hydrogen ratio but also to the sequence of the gas flow feed.

Generally, SFG spectra from surfaces not only provide the essential spectral signatures of the adsorbate, but are also coupled to the electronic structure of the substrate in the form of nonresonant SFG (nr-SFG) signals. A surface SFG spectrum is thus generated by the interference between the adsorbate vibrational spectrum and the substrate nr-SFG signal. It has been shown by Dreesen et al. that nr-SFG is directly coupled to the surface electronic density of states (DOS) and the electronic band structure of the substrate.[22] Somorjai et al. had reported modulations in nr-SFG signals from an Fe(111) substrate by various gaseous adsorbates and speculated the nr-SFG to be related to the substrate work functions under various precoverages.[21] In this article, we report on the sensitivity of nr-SFG signals to the gas feed ratios and feed sequences and have demonstrated correlations between the substrate nr-SFG signals and catalytic ethane generation. We anticipate the use of nr-SFG as a new probe for catalytic activities of metal surfaces and surface electronic structures.

EXPERIMENTAL SECTION

Total internal reflection (TIR)−SFG was used to study the surface of a high-surface-area catalyst powder. The TIR−SFG cell was constructed in-house and was built of stainless steel with gas inlet/outlet ports and heating capabilities, as shown in Figure 1. Approximately 20 mg of pure (≥99.9%) Pt powder (0.5−1.2 μm, Sigma-Aldrich) was pressed to a 5 mm diameter pellet (3.9×10^{-3} m^2/g) at 5000 psi using a hydraulic pellet press (Specac) and then calcined in air at 500 °C for 2 h to remove possible organic impurities. The pellet was then kept

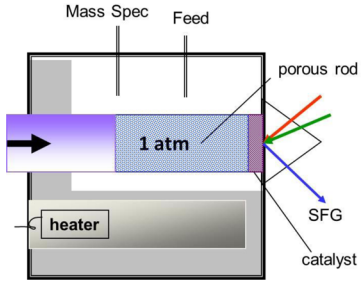

Figure 1. Schematic of the SFG reactor cell used in the SFG−MS experiments.

dx.doi.org/10.1021/cs500109b | ACS Catal. 2014, 4, 1964−1971

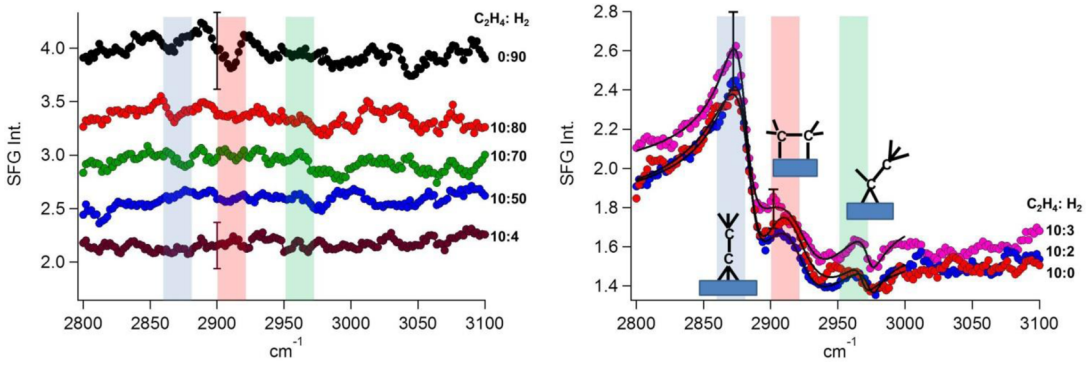

Figure 2. Normalized SFG spectra of Pt surface precovered with H_2 and for various C_2H_4/H_2 feed ratios. The left graph shows SFG spectra at high H_2 flows or lower C_2H_4/H_2 ratios (<3:1) where no hydrocarbon signatures are observed. The right graph shows SFG spectra for higher C_2H_4/H_2 ratios (>3:1) (with clear signatures of surface hydrocarbonaceous intermediates of ethylidyne (~2880 cm-1) indicated by the blue band, di-σ-ethylene (~2910 cm^{-1}) indicated by the red band, and a CH_3 asymmetric stretch mode at ~2950 cm^{-1} indicated by the green band) arising from ethylidene or ethylidyne. The SFG spectral baselines in both the left and right graphs are not offset but indicate real SFG intensity acquired. The baseline shifts indicate modulation of the nonresonant SFG signal generated by the Pt substrate at different reactant feed ratios. The solid lines through the data are fits to eq 1. Error bars are also indicated for some of the spectra.

firmly pressed against the sapphire prism in a home-built TIR–SFG cell using a stainless steel porous rod. A feed flow was set up inside the cell by allowing the gases to flow in through an entry port controlled by a mass flow controller and flow out through an exit port on the housing, which was connected to a mass spectrometer.

Prior to SFG experiments, the calcined Pt pellet placed inside the cell was reduced under an H_2/He environment at 250 °C for 1 h, followed by cooling to room temperature under He. A number of such calcined/reduced pellets were used for various SFG–MS experiments. Details of the SFG optical setup are described elsewhere.[32] Briefly, this nonlinear optical spectroscopic technique employs two laser beams (1 ns pulses at 10 Hz): one that is fixed at a visible wavelength of 532 nm (generated by Spectra Physics Quanta Ray Pro) and the other that is tunable in the mid-IR region (2800–3200 cm^{-1}). The tunable mid-IR wavelength is generated by stimulated Raman scattering of a doubled-Nd:YAG pumped dye laser (Lumonics laser: DCM dye) in a multipass H_2 cell. A portion of the output of the doubled-Nd:YAG laser was used as the visible light source. The visible and mid-IR (1.5 mJ/pulse) beams are then focused to spot sizes of ~100 μm and are overlapped at the catalyst pellet surface under the sapphire prism at an angle greater than the critical angle characteristic for the Pt/sapphire interface (see Figure 1). The emerging SF signals from the catalyst surface are then detected using a photomultiplier tube and gated electronics. The polarization combination for the SFG, visible, and mid-infrared beams is chosen to be ppp (with respect to the incident plane of the catalyst) because maximum SF intensity is obtained from the catalyst surface with this polarization configuration. A spectrum is obtained by recording SFG intensities at different IR wavelengths.

In a typical SFG–MS experiment, a particular ratio of C_2H_4/H_2/He flow rate was allowed to flow continuously through the SFG reactor cell at room temperature and ~1 atm pressure. The total flow rate of gases was kept constant at 100 standard cubic cm/min (sccm), and He was used as a carrier gas. The ion currents for C_2H_4, H_2, He, and C_2H_6 were simultaneously recorded with the MS for every flow ratio. Sufficiently long times were allowed for reactant gases to establish equilibrium inside the reactor cell, as determined by the MS ion currents. Subsequently, SFG spectra were recorded in the spectral window between 2800 and 3100 cm^{-1}. IR intensity spectra were also recorded to account for drifts in laser intensity and were used to normalize the SFG spectra.

SFG–MS experiments were performed for a series of different feed gas ratios for two different feed injection sequences. In the first set, experiments were performed on calcined/reduced Pt with an initial flow of H_2-rich gas feed (90 sccm H_2/10 sccm He) and no C_2H_4. Subsequently, C_2H_4 was injected at a constant rate of 10 sccm while the H_2 flow was decreased in a stepwise manner, keeping the total flow rate constant at 100 sccm (adjusted by He flow rate). In the second set, experiments were performed on a freshly calcined/reduced catalyst with a C_2H_4 rich gas feed (10 sccm C_2H_4/90 sccm He) with no H_2 to start with and subsequently increasing the H_2 flow and maintaining a constant flow of C_2H_4 at 10 sccm. In this way, the effects of variable gas feed ratios and different sequences were studied. Simultaneously, the effects on ethane generation were followed as a function of ion current recorded by the MS.

RESULTS

All the SFG spectra obtained for different feed ratios and feed sequences have been normalized by their corresponding IR input power spectra and were fitted to the Lorentzian equation:

$$I_{SFG} \propto |\chi^{(2)}|^2 = \left| A_{NR} e^{i\varphi_{NR}} + \sum_{j=1}^{N} \frac{A_j e^{i\varphi_j}}{\omega_j - \omega - i\Gamma_j} \right|^2 \quad (1)$$

Here, I_{SFG}, is the SFG intensity, $\chi^{(2)}$ is the nonlinear second-order susceptibility, ω is the frequency of the IR laser light, ω_j is the resonance frequency and Γ_j is the line-width of the jth vibrational mode of the adsorbate species. A_{NR} and A_j are the amplitudes of the nonresonance and resonance, respectively. ϕ_{NR} and ϕ_j are the phases associated with the nonresonant and resonant second-order susceptibilities, respectively, which contribute to the SFG line-shape. A detailed discussion on the effect of phases on SFG spectral line-shape can be found in the Supporting Information. Various SFG spectral observables—amplitudes of the resonances, peak frequencies, and nonresonant amplitudes—were extracted by fitting all data sets. These observables were monitored as a function of C_2H_4/H_2 ratios in an attempt to understand the effects of gas feed

dx.doi.org/10.1021/cs500109b | ACS Catal. 2014, 4, 1964–1971

sequences and flow ratios on catalytic hydrogenation of ethylene. In all the SFG measurements, the relative measured error is ±5% of the spectral intensity. Therefore, the oscillations observed in the 0:90 C_2H_4/H_2 data in Figure 2 (top graph), lie within the uncertainty of the measurement, whereas in the 10:3 C_2H_4/H_2 data in Figure 2 (bottom graph), the intensity of the hydrocarbon feature at 2880 cm^{-1} is much greater than the error bar. Peak assignments made in this article are based on previous studies.[7,8,12,14,15,17−20,24,33,34] The results for our SFG−MS experiments with varying feed sequences and ratios have been categorized into the following three parts: SFG of H_2-precovered Pt, SFG of C_2H_4-precovered Pt, and the MS results of hydrogenation reaction under various conditions of feed sequences and ratios.

Pt Surface Precovered with Hydrogen. Starting with low C_2H_4/H_2 ratios and a subsequent increase in the ratios (as shown in Figure 2), the hydrocarbon spectral features (indicated by colored bands) start to appear only at C_2H_4/H_2 ratios of 3:1 and higher. Flow ratios lower than 3:1 (higher H_2 flows) do not show any distinct hydrocarbon signature within our instrument signal-to-noise range. The spectral feature in the range of 2880−2885 cm^{-1} (blue band) has been assigned to the CH_3 symmetric stretch of ethylidyne (Pt_3CCH_3), and the feature within 2905−2915 cm^{-1} (red band), to CH_2 symmetric stretch of di-σ-ethylene,[19,20] which are observed at C_2H_4/H_2 ratios higher than 3:1. Under H_2-poor conditions, the feature at 2950 cm^{-1} (green band) is assigned to a CH_3 asymmetric stretch mode that may arise from ethylidyne (Pt_3CCH_3) or from ethylidene (Pt_2CHCH_3) intermediates.[18] The 2950 cm^{-1} feature could also represent the CH_3 asymmetric stretch mode of an ethyl ($PtCH_2CH_3$) intermediate; however, this assignment is ruled out at high C_2H_4/H_2 ratios because its formation requires low C_2H_4/H_2 ratios (a large number of surface-adsorbed H). Under H_2-rich feeds (ratios lower than 3:1), for which the conversion of ethylene is higher, ethyl is said to be the primary intermediate; however, at room temperatures, the ethyl species is very difficult to detect because it readily undergoes β-hydride elimination to form di-σ-ethylene and adsorbed hydrogen.[8] Few groups have been able to detect the ethyl intermediate under conditions of high H_2 pressures[13] and low temperatures (~190 K),[18] but the ethyl features could not be detected in our experiments at room temperature conditions and at the lower C_2H_4/H_2 ratios (<3:1). Features above 2990 cm^{-1} have been reported in earlier RAIRS studies to originate from species such as vinyl and vinylidene or even π-ethylene.[18]

In Figure 3, variation of some of the observed hydrocarbonaceous species is shown as a variation in amplitudes of the SFG spectral features as a function of increasing C_2H_4/H_2 ratios. We observe that the amplitudes of most of the hydrocarbonaceous species increase by ~3−4 times at a 3:1 C_2H_4/H_2 ratio. Another interesting feature to note about the normalized SFG spectra is the significant variation in the spectral baseline intensities as a function of the C_2H_4/H_2 feed ratios.

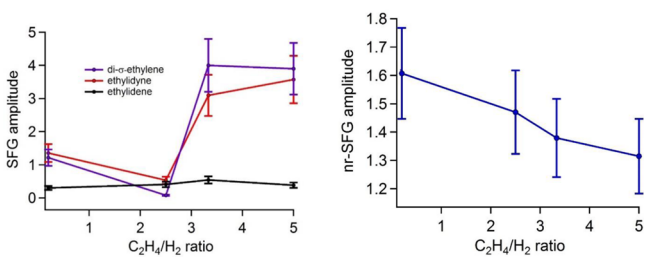

Figure 3. Resonant SFG amplitudes (left graph) of the various surface hydrocarbon intermediates and the nonresonant SFG amplitudes of the Pt surface (right graph) shown were monitored as a function of increasing C_2H_4/H_2 ratios at a H_2-precovered Pt surface.

This baseline is attributed to nr-SFG photons arising as a result of electronic excitations in the metal substrate.[22] No SFG signal is detected from a calcined/reduced bare Pt metal, and the nr-SFG is largest when clean Pt is exposed to a H_2-rich environment. As shown in Figure 3, with a subsequent increase in the C_2H_4/H_2 ratio (decreasing H_2), the nr-SFG amplitude decreases as the hydrocarbonaceous species begin to appear on the Pt surface.

Pt Surface Precovered with Ethylene. SFG spectra were recorded for C_2H_4-precovered Pt, starting with high C_2H_4/H_2 feed ratios (10:1 to 2:1) (Figure 4, top graph) and subsequently followed by lower feed ratios (<2:1) (Figure 4, bottom graph). The presence of hydrocarbonaceous species is evident in the SFG spectra of the C_2H_4-precovered Pt surface and at high C_2H_4/H_2 ratios (>2:1). Features characteristic of surface ethylidyne (Figure 4, blue band) and di-σ-ethylene (Figure 4, red band) and for CH_3 asymmetric stretch (green band) arising from ethylidyne or ethylidene are readily observed at high C_2H_4/H_2 ratios, as was observed at high C_2H_4/H_2 ratios for H_2-precovered Pt. An additional spectral feature is observed at 2850 cm^{-1}, characteristic of CH_3 symmetric stretch of ethylidene (Pt_2CHCH_3),[15,18] thus confirming its presence as a prominent surface intermediate along with ethylidyne and di-σ-ethylene in C_2H_4-rich conditions. A subsequent increase in H_2 flow rates over C_2H_4- precovered Pt leads to partial removal of the hydrocarbonaceous species, as indicated by decreasing hydrocarbon spectral amplitudes. The removal of surface hydrocarbons is, however, only partial because there are reminiscent features of the hydrocarbonaceous species even at higher H_2 flows, as can be seen in Figure 4 (bottom graph). The nr-SFG amplitude increases with decreasing C_2H_4/H_2 feed ratios but stays significantly lower than in the case of H_2-precovered Pt. Figure 5 shows the amplitudes of the hydrocarbonaceous peaks and the nr-SFG as a function of C_2H_4/H_2 ratios. A decrease in the hydrocarbon spectral amplitudes and an increase in the nr-SFG are observed, similar to the H_2-precovered case, albeit the changes observed are not as abrupt as the appearance of hydrocarbons and decrease in nr-SFG amplitudes as for the H_2 preconditions.

Mass Spectrometry of Ethane Generation. As shown in Figure 6, ethane production was followed at every feed ratio for both the Pt preconditions by recording the mass spectrometer ion currents of the evolved ethane gas during the reaction. The highest ethane production was observed in the case that Pt was precovered with H_2. With increasing C_2H_4/H_2 ratios (decreasing H_2 flows), ethane production decreased (Figure 6, open blue circles) as a result of deposition of hydrocarbonaceous intermediates on the Pt active sites. Subsequent increase of H_2 flow over Pt (Figure 6, solid blue circles) led to an increased but irreversible ethane production, thereby suggesting partial deactivation of the Pt active sites by the hydrocarbonaceous species already deposited by the previous cycle of high C_2H_4/H_2 feed. These intermediates evidently could not be removed from the surface by a reverse H_2 flow, possibly because of transformation of the hydrocarbonaceous species to carbonaceous species such as coke, poly aromatics, etc., which could not be detected by SFG spectroscopy. As shown in Figure 6, in the case of C_2H_4-precovered Pt, ethane production

dx.doi.org/10.1021/cs500109b | ACS Catal. 2014, 4, 1964−1971

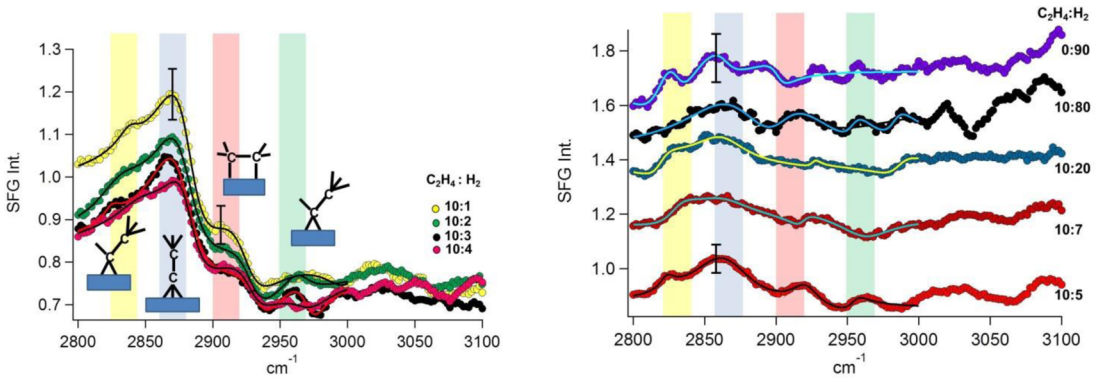

Figure 4. Normalized SFG spectra are shown for C_2H_4-precovered Pt at various feed ratios starting with high C_2H_4/H_2 ratios. The left graph shows the SFG spectra for high C_2H_4/H_2 ratios between 10:1 and 10:4, where signatures for hydrocarbonaceous intermediates of ethylidyne (blue), di-σ-ethylene (red), and ethylidene (yellow and green) are clearly observed. The right graph shows SFG spectra for sequentially decreasing C_2H_4/H_2 ratios from 2:1 up to 0:90. The SFG spectral amplitudes of the hydrocarbonaceous intermediates observed at higher C_2H_4/H_2 feed ratios significantly decrease with increasing H_2 flows, but never disappear, even in the absence of C_2H_4 in the feed. Variation in the SFG spectral baseline indicates modulation in nr-SFG signal amplitudes generated by the Pt substrate at different reactant feed ratios. The nr-SFG amplitude increases with decreasing C_2H_4/H_2 feed ratios but stays significantly lower than in the case of H_2-precovered Pt (see Figure 2). The solid lines through the data are fits to eq 1.

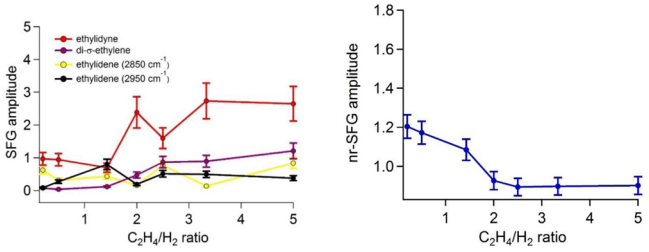

Figure 5. Resonant SFG amplitudes (left axis) of the various surface hydrocarbon species and the nonresonant SFG amplitude of the Pt substrate (right axis) shown were monitored as a function of decreasing C_2H_4/H_2 ratios for C_2H_4-precovered Pt. Note that this experiment was performed with a gradual decrease in the C_2H_4/H_2 ratios (i.e., right to left).

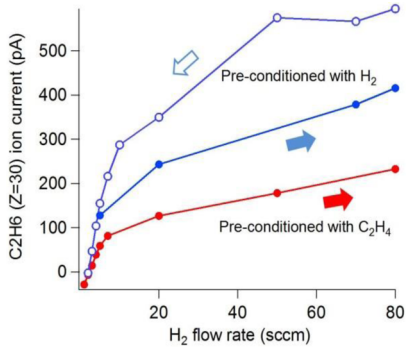

Figure 6. MS ion currents of ethane (mass 30) for both high H_2 and high C_2H_4 precoverages as a function of H_2 flow rates. The blue curves are for the H_2-precovered Pt; the open circles are for the high-to-low H_2 flows, whereas the closed circles are for the subsequent reverse flow experiment. The arrows indicate the directions of the feed ratio sequences. The red curve is for the C_2H_4-precovered Pt, and the arrow indicates the direction of the experiment. The ion current has been normalized by the catalyst weights in every experiment.

was at least three times less than in the case of H_2-precovered Pt at the highest H_2 flow rate, thus suggesting partial deactivation of the catalyst as a result of formation of surface intermediates that cannot be removed easily from the surface sites.

DISCUSSION

The reactant gas feed sequence and initial conditions of Pt govern the formation of hydrocarbonaceous surface intermediates and the overall catalytic hydrogenation process. This is shown by the fact that SFG spectra for the two preconditions (C_2H_4 and H_2) of Pt are not identical at a given C_2H_4/H_2 feed ratio. Starting with low C_2H_4/H_2 ratios (0:90) and subsequently decreasing H_2 flows, over H_2-pretreated Pt, the SFG spectral signatures for hydrocarbonaceous species of ethylidyne (Pt_3CCH_3), di-σ-ethylene ($Pt_2CH_2CH_2$), and ethylidene (Pt_2CHCH_2) start to appear abruptly only at C_2H_4/H_2 ratios around 3:1 and higher; no SFG resonances were observed at lower C_2H_4/H_2 feed ratios (<3:1) within the instrument signal-to-noise. Simultaneous monitoring of MS ion current for the ethylene hydrogenation product, ethane (mass 30), as a function of increasing C_2H_4/H_2 ratios over H_2-pretreated Pt indicates that more ethane is generated when C_2H_4/H_2 ratios are lower than 3:1, above which the hydrocarbonaceous intermediates start appearing in the SFG spectra. Therefore, the presence of an excess amount of adsorbed hydrogen on the Pt surface is crucial for efficient catalytic hydrogenation of ethylene to produce ethane.

In the case of C_2H_4-pretreated Pt, for which the experiments begin with high C_2H_4/H_2 ratios (10:1), the SFG spectral signatures of hydrocarbonaceous surface intermediates are observed at the very onset of the experiment, and the MS ion current of ethane is observed to be very low, suggesting inefficient ethylene hydrogenation. With increasing H_2 flow over C_2H_4-pretreated Pt, the SFG spectral signatures of the hydrocarbonaceous species diminish but do not disappear completely, even in the absence of C_2H_4 and high flows of H_2. This observation of an abrupt appearance of CCH_3 features in the case of increasing C_2H_4 pressures on H_2-pretreated Pt and slow disappearance of CCH_3 in the case of increasing H_2 pressures on C_2H_4-pretreated Pt is, in fact, in accordance with the in situ IR transmission studies of ethylene hydrogenation by Rekoske et al.[27] and with the microkinetic modeling studies by Vlachos et al.,[26] where they observe CCH_3 species only at

dx.doi.org/10.1021/cs500109b | ACS Catal. 2014, 4, 1964−1971

C_2H_4/H_2 ratios of 5:1 but not at 0.5:1 for the same precondition.

The sudden appearance of ethylidyne SFG features at C_2H_4/H_2 > 3:1 from a relatively featureless spectrum at C_2H_4/H_2 < 3:1, is speculated to be caused by the abrupt change in surface coverage of H atoms adsorbed on the Pt. At a high surface coverage of H_2 on Pt, conversion of adsorbed ethylene (π-C_2H_4) to ethane is the more preferred pathway (because of an abundance of the reactive surface-adsorbed H atoms) than the pathway that leads to formation of surface ethylidyne. However, at C_2H_4/H_2 ratios higher than 3:1, the surface coverage is primarily dominated by π-C_2H_4, and formation of ethylidyne becomes the primary pathway (see Figure 8).

In the case of C_2H_4-pretreated Pt, for which the adsorbed π-C_2H_4 has a maximum surface coverage to begin with, formation of ethylidyne is the more preferred pathway in the absence of H_2 (or low H_2). For this case, we may speculate the formation of other carbonaceous species (not detected within our SFG spectral range) on the Pt surface. These species could be the cause of the marked weakening of the ethylidyne SFG feature with an abundance of H_2 flow. This is further corroborated by the relatively lower MS ion current for the generated ethane at all feed ratios, which suggests inefficient ethylene hydrogenation at the C_2H_4-pretreated Pt surface in comparison with H_2-pretreated Pt. In fact, we find that ethane generation is at least 3 times less in the case of C_2H_4-pretreated Pt than it is in the case of H_2-pretreated Pt. It is also likely that the hydrocarbons on the surface readily transform into carbonaceous intermediates such as coke, poly aromatics, etc. which are difficult to remove only with a reverse H_2 flow and not generally detected by SFG spectroscopy. These observations suggest that the outcome of a catalytic hydrogenation process at room temperatures and pressures is a sensitive function of catalyst pretreatment and reactant gas feed sequence—factors that affect competitive adsorption of the reactants, intermediates, and products on the catalyst surface. Under H_2-rich conditions, where Pt surface sites are adsorbed primarily by H atoms prior to C_2H_4 exposure, ethylene hydrogenation is observed to be a very efficient process. Once the surface gets exposed to C_2H_4, the hydrocarbons on the surface block the catalytic sites and reduce the efficiency of the process. Under C_2H_4-rich conditions prior to exposure to H_2, the hydrocarbons and carbonaceous species block most of the surface sites at the very onset of the hydrogenation process, thus making the process an inefficient one to begin with. This explains the disparity in the generation of ethane with the two different catalyst preconditions and also in the SFG spectra with the two different feed sequences.

The hydrocarbon intermediates observed at both preconditions are observed mostly at high C_2H_4/H_2 feed ratios. The feature at 2880−2885 cm^{-1} has been assigned to the CH_3 symmetric stretch of ethylidyne, as observed by other groups.[19,20] The feature observed in the region of 2905−2915 cm^{-1} has been assigned to di-σ-ethylene (Pt−CH_2 symmetric stretch), per earlier studies by Cremer et al.[20] The feature at 2950−2960 cm^{-1} is likely due to the asymmetric stretch of the CH_3 moiety of ethylidene (Pt_2CHCH_3), as reported by Cremer et al.[18] Furthermore, a feature observed at 2850 cm^{-1} has been assigned to the CH_3 symmetric stretch mode of ethylidene (Pt_2CHCH_3), also reported by Cremer et al.[18] This feature at 2850 cm^{-1} is more pronounced in the case of C_2H_4-precovered Pt, thus indicating the prominence of ethylidene as an important intermediate at the Pt surface at higher C_2H_4/H_2 ratios. At lower C_2H_4/H_2 ratios, a feature due to an ethyl intermediate ($PtCH_2CH_3$), which is the primary precursor to ethane formation according to earlier reports,[20] is expected in the SFG spectra at 2950−2960 cm^{-1}. However, it is difficult to detect the ethyl intermediate because it is readily convertible to di-σ-ethylene at room temperature and pressures of the feed gases. Features above 2990 cm^{-1} could be that of the CH_2 symmetric stretch of other ethylene decomposition products, such as vinyl and vinylidene, as characterized by Cremer et al.[18]

In addition to the effects on hydrocarbon SFG resonances and the MS ion currents, the feed sequence and ratios have also been observed to have a large effect on the nonresonance SFG intensities that originate from the Pt catalyst surface. The nr-SFG signal typically seen as a background in a surface SFG spectrum is shown to be markedly sensitive to the adsorption of H atoms on the Pt metal surface (details in Supporting Information). The nr-SFG amplitude was, however, observed to be the least in the presence of the surface hydrocarbonaceous intermediates. It has been reported earlier that adsorption of different molecules on metal substrates can either increase or decrease the nr-SFG. For instance, H_2 enhances the nr-SFG of the Fe(111) surface, and O_2 reduces the intensity drastically.[21] It was shown in earlier SHG studies of O_2 on Re(0001)[35] or of H_2 on a Pt electrode[36] that electron-donating (-withdrawing) adsorbates decreased (increased) the work function of the metal substrate, resulting in an increase (decrease) in nonresonant SH signal. SFG experiments with dodecanethiol adsorbed on various metal substrates (Pt, Au, Ag) by Dreesen et al. demonstrated the DOS of the metal and the position of metallic d-bands with respect to the Fermi level.[22]

It may be noted that adsorption of molecules that cause lowering (raising) of the Fermi level can increase (reduce) nr-SFG intensities under our experimental conditions. We observed large nr-SFG intensities from Pt only in the presence of H_2, suggesting a shift in the electronic band structure upon adsorption of H on Pt surface. As shown in Figure S3 (see the Supporting Information), in our sequential feed experiments, the H_2-pretreated Pt shows high nr-SFG signal amplitudes that decrease with increasing hydrocarbonaceous adsorbates such as ethylidyne, di-σ-C_2H_4, and ethylidene. C_2H_4-pretreated Pt, which shows the presence of hydrocarbonaceous intermediates at the very onset of the experiments, shows very low nr-SFG signal amplitude to begin with. With decreasing C_2H_4/H_2 ratios, the nr-SFG amplitudes increase but are significantly lower than the amplitudes observed for H_2-precovered Pt. These observations suggest that there is competitive adsorption between H_2 and the hydrocarbonaceous species on the Pt surface. This suggests that adsorption of hydrocarbonaceous species raises the Pt surface Fermi level, causing a decrease in the nr-SFG signal intensity, whereas adsorbed hydrogen lowers the surface Fermi level, thereby increasing the nr-SFG intensity. The H_2-pretreated Pt generally shows higher nr-SFG intensities than C_2H_4-pretreated Pt, irrespective of the feed ratios. This may be explained by a scenario in which in the case of C_2H_4-pretreated Pt, the surface hydrocarbonaceous intermediates may have transformed into irremovable and site-deactivating carbonaceous species such as coke or poly aromatics, which keep the Fermi level of the Pt surface high. Extensive DFT calculations to quantify the effects of H_2 and hydrocarbonaceous adsorbates on the d-band structure of the Pt metal surface are underway, but they are out of the scope of this paper.

We observed in our sequential feed experiments that nr-SFG amplitudes can be directly correlated to catalytic ethane production within a given catalyst precondition: the larger the nr-SFG amplitudes, hte greater the MS ion current of ethane. As can be seen in Figure 7, the MS ion current of

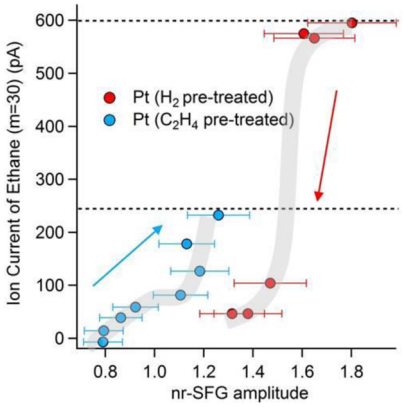

Figure 7. Correlation between ethane generation and observed nonresonant SFG amplitudes for two different preconditions of Pt powder catalyst is shown here. The arrows indicate the direction of the experiments with respect to the C_2H_4/H_2 feed ratios. The blue arrow indicates the direction in which the C_2H_4/H_2 ratio was decreased (increasing H_2 flows) on C_2H_4-pretreated Pt. The red arrow indicates the direction in which the feed ratio on H_2-pretreated Pt was increased (decreased H_2 flows). The solid gray lines through the curves are a guide to the eye. In both pretreatments, it is observed that the MS ion current of ethane tends to be low when the nr-SFG amplitudes are low, and the ion currents are high when nr-SFG amplitudes are high, suggesting nr-SFG to be a sensitive indicator of catalyst activity.

ethane tends to be low when the nr-SFG amplitudes are low at high C_2H_4/H_2 feed ratios and vice versa, irrespective of the pretreatment. However, it is observed that for C_2H_4-pretreated Pt, both the nr-SFG and MS ion current for ethane stay significantly lower than H_2-pretreated Pt, suggesting partial deactivation of the Pt active sites by the strongly bound hydrocarbonaceous and carbonaceous intermediates in the case of the C_2H_4-pretreated Pt. It can also be seen from Figure 7 that the H_2-pretreated Pt generates at least 3 times more ethane than what C_2H_4-pretreated Pt does. This indicates nr-SFG to be demonstrably a very sensitive probe for the electronic structure and the catalytic activity of the metal surface, as a function of adsorbed H_2 and hydrocarbonaceous species. Further SFG experiments are being conducted to directly address and monitor the Pt−H SFG resonance that typically is observed around 2050 cm^{-1} to understand the effects on nr-SFG as a function of H adsorption on Pt. DFT calculations are also underway to correlate the electronic structure at metal surfaces, nr-SFG amplitudes, and their relation to the effective catalytic activity of the metal surface. Keeping in mind the C_2H_4/H_2 ratio and feed sequence effects on the SFG spectra and the MS, two distinct pathways may exist for ethylene conversion (see Figure 8) at room temperature and pressure, depending on the preconditions of the catalyst as it has been known, but also it seems possible to cross over into the other pathway by tuning the C_2H_4/H_2 ratios.

CONCLUSION

We have performed SFG−MS experiments on pelletized Pt powder with sequential reactant feeds and ratios to understand

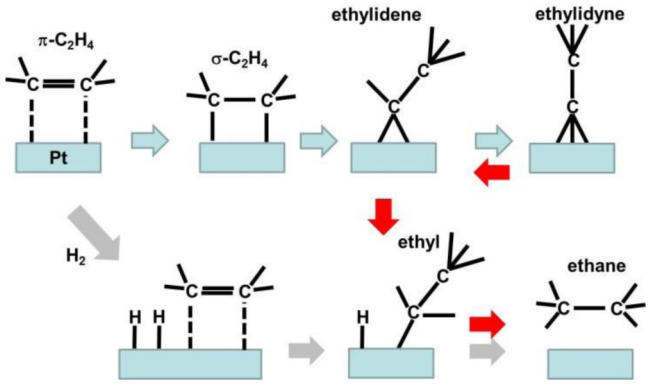

Figure 8. Schematic of the reaction mechanisms involved in the catalytic hydrogenation (and decomposition) of ethylene. For similar reaction paths for this reaction, see references 15, 26. The top half of the reaction sequence indicates decomposition of ethylene on a Pt surface in the absence of H_2. The bottom half depicts the reaction sequence involved in ethylene hydrogenation over the Pt metal in the presence of excess H_2. The red arrows indicate the scenario in which hydrogenation to ethane takes place in the presence of H_2 after ethylene has decomposed into various hydrocarbonaceous species in a H_2-starved reaction.

their effects on the surface intermediates, substrate electronic structure and the overall ethylene hydrogenation reaction. We have demonstrated that the competitive adsorption between hydrogen and surface hydrocarbon species causes marked sensitivity to the Pt surface preconditioning. In the case of the H_2-pretreated Pt, the overall ethylene hydrogenation reaction produced more ethane at low C_2H_4/H_2 feed ratios as compared with the C_2H_4-pretreated Pt. Ethylidyne, ethylidene, and di-σ-ethylene are the primary hydrocarbonaceous species that are detected at the Pt surface using SFG spectroscopy at high C_2H_4/H_2 ratios. For C_2H_4-pretreated Pt, SFG spectral signatures of the hydrocarbonaceous intermediates appear at the onset of the experiment with high C_2H_4/H_2 feed ratios but gradually decrease with decreasing feed ratios, although not disappearing completely with high H_2 flows. Because the presence of hydrocarbonaceous species such as ethylidyne and di-σ-ethylene on Pt evidently reduces ethylene hydrogenation and the nr-SFG intensities, these surface species seem to play a significant role in the overall mechanism of catalytic hydrogenation of ethylene to ethane. The feed sequence evidently plays a major role in deciding the outcome of the hydrogenation reaction by affecting the competitive adsorption of the reactants, intermediates, and products on the catalyst surface.

The nonresonant SFG intensities generated by the metal catalyst substrate are demonstrated to be sensitive to the pretreatment of the catalyst, the sequence of reactant feeds, and ratios. The nr-SFG is enhanced to large extents in the presence of H_2-rich conditions, but it is hampered in the presence of C_2H_4; the H_2-pretreated Pt has overall high nr-SFG signal amplitudes as compared with C_2H_4-pretreated Pt. The nr-SFG amplitudes and the ethane generation are correlated within a given precondition of the catalyst, in which a high nr-SFG signal is indicative of high ethylene conversion efficiency. Low nr-SFG amplitudes and therefore low ethane generation due to th presence of hydrocarbonaceous intermediates on the Pt surface is difficult to recover because the hydrocarbons presumably transform into carbonaceous products such as coke that are difficult to remove from the surface and are difficult to predict with resonant SFG spectroscopy. Further

dx.doi.org/10.1021/cs500109b | ACS Catal. 2014, 4, 1964−1971

SFG experiments are underway to understand the role of H_2 adsorption on Pt on the enhanced nonresonant SFG amplitudes. Surface DFT calculations are also being performed to establish nr-SFG as a quantitative probe for catalytic activity and electronic structure of metal surfaces.

■ ASSOCIATED CONTENT

Supporting Information

Effect of phase of vibrational modes on SFG line-shape; effect of H_2 adsorption on Pt on nr-SFG intensity; comparison of nr-SFG intensities under different preconditions, gas feed sequences, and ratios. This material is available free of charge via the Internet at http://pubs.acs.org.

■ AUTHOR INFORMATION

Corresponding Author

*E-mail: avishek01@gmail.com.

Present Addresses

[†]School of Physical and Mathematical Sciences, Nanyang Technological University, 50 Nanyang Avenue, Singapore 639798.

[‡]Department of Chemistry, Massachusetts Institute of Technology, 77 Massachusetts Avenue, Cambridge, MA 02139, United States.

Notes

The authors declare no competing financial interest.

■ ACKNOWLEDGMENTS

All the authors would like to acknowledge Steve P. Rucker, Yogesh Joshi and Sumathy Raman for stimulating discussions.

■ REFERENCES

(1) Lloyd, L. *Handbook of Industrial Catalysts*; Springer: New York, 2011.
(2) von Wilde, M. P. *Eur. J. Inorg. Chem.* **1874**, *7*, 352−357.
(3) Horiuti, J.; Miyahara, K. *NBS-NSRDC*; U.S. Government Printing Office: Washington D.C., 1968, Vol. *13*; p 62.
(4) Bond, G. C.; Phillipson, J. J.; Wells, P. B.; Winterbottom, J. M. *Trans. Faraday Soc.* **1964**, *60*, 1847−1864.
(5) Bond, G. C. *Trans. Faraday Soc.* **1956**, *52*, 1235−1244.
(6) Horiuti, I.; Polanyi, M. *Trans. Faraday Soc.* **1934**, *30*, 1164−1172.
(7) Kesmodel, L. L.; Dubois, L. H.; Somorjai, G. A. *J. Chem. Phys.* **1979**, *70*, 2180−2188.
(8) Zaera, F.; Somorjai, G. A. *J. Am. Chem. Soc.* **1984**, *106*, 2288−2293.
(9) Ibach, H.; Mills, D. *Electron Energy Loss Spectroscopy and Surface Vibrations*; Academic Press: New York, 1982.
(10) Steininger, H.; Ibach, H.; Lehwald, S. *Surf. Sci.* **1982**, *117*, 685−698.
(11) Backman, A. L.; Masel, R. I. *J. Vac. Sci. Technol. A* **1991**, *9*, 1789−1792.
(12) Ko, M. K.; Frei, H. *J. Phys. Chem. B* **2004**, *108*, 1805−1808.
(13) Wasylenko, W.; Frei, H. *J. Phys. Chem. B* **2005**, *109*, 16873−16878.
(14) Mohsin, S. B.; Trenary, M.; Robota, H. J. *J. Phys. Chem.* **1991**, *95*, 6657−6661.
(15) Deng, R. P.; Herceg, E.; Trenary. *Surf. Sci.* **2004**, *560*, L195−L201.
(16) Chesters, M. A.; McCash, E. M. *Surf. Sci.* **1987**, *187*, L639−L641.
(17) Malik, I. J.; Agrawal, V. K.; Trenary, M. *J. Chem. Phys.* **1988**, *89*, 3861−3869.
(18) Cremer, P.; Stanners, C.; Niemantsverdriet, J. W.; Shen, Y. R.; Somorjai, G. *Surf. Sci.* **1995**, *328*, 111−118.
(19) Cremer, P. S.; Somorjai, G. A. *J. Chem. Soc., Faraday Trans.* **1995**, *91*, 3671−3677.
(20) Cremer, P. S.; Su, X.; Shen, Y. R.; Somorjai, G. A. *J. Am. Chem. Soc.* **1996**, *118*, 2942−2949.
(21) Westerberg, S.; Wang, C.; Chou, K.; Somorjai, G. A. *J. Phys. Chem. B* **2004**, *108*, 6374−6380.
(22) Dreesen, L.; Humbert, C.; Celebi, M.; Lemaire, J. J.; Mani, A. A.; Thiry, P. A.; Peremans, A. *Appl. Phys. B: Laser Opt.* **2002**, *74*, 621−625.
(23) Cremer, P. S.; Su, X. C.; Shen, Y. R.; Somorjai, G. A. *Catal. Lett.* **1996**, *40*, 143−145.
(24) Cremer, P. S.; Su, X. C.; Somorjai, G. A.; Shen, Y. R. *J. Mol. Catal. A: Chem.* **1998**, *131*, 225−241.
(25) Somorjai, G. A.; McCrea, K. R. *Adv. Catal.* **2000**, *45*, 385−438.
(26) Salciccioli, M.; Chen, Y.; Vlachos, D. G. *Ind. Eng. Chem. Res.* **2011**, *50*, 28−40.
(27) Rekoske, J. E.; Cortright, R. D.; Goddard, S. A.; Sharma, S. B.; Dumesic, J. A. *J. Phys. Chem.* **1992**, *96*, 1880−1888.
(28) Podkolzin, S. G.; Watwe, R. M.; Yan, Q. L.; de Pablo, J. J.; Dumesic, J. A. *J. Phys. Chem. B* **2001**, *105*, 8550−8562.
(29) Neurock, M.; van Santen, R. A. *J. Phys. Chem. B* **2000**, *104*, 11127−11145.
(30) Chen, Y.; Vlachos, D. G. *J. Phys. Chem. C* **2010**, *114*, 4973−4982.
(31) Yeganeh, M. S.; Dougal, S. A.; Silbernagel, B. G. *Langmuir* **2006**, *22*, 637−641.
(32) Yeganeh, M. S.; Dougal, S. M.; Polizzotti, R. S.; Rabinowitz, P. *Thin Solid Films* **1995**, *270*, 226−229.
(33) Cremer, P. S.; Su, X. C.; Shen, Y. R.; Somorjai, G. A. *J. Phys. Chem.* **1996**, *100*, 16302−16309.
(34) Ohtani, T.; Kubota, J.; Kondo, J. N.; Hirose, C.; Domen, K. *J. Phys. Chem. B* **1999**, *103*, 4562−4565.
(35) Rosenzweig, Z.; Asscher, M. *Surf. Sci.* **1988**, *204*, L732−L738.
(36) Corn, R. M.; Higgins, D. A. *Chem. Rev.* **1994**, *94*, 107−125.